

# Liquid Extraction Surface Analysis Mass Spectrometry Coupled with Field Asymmetric Waveform Ion Mobility Spectrometry for Analysis of Intact Proteins from Biological Substrates

Joscelyn Sarsby,<sup>†</sup> Rian L. Griffiths,<sup>†</sup> Alan M. Race,<sup>‡</sup> Josephine Bunch,<sup>‡,§</sup> Elizabeth C. Randall,<sup>†</sup> Andrew J. Creese,<sup>†</sup> and Helen J. Cooper<sup>\*,†</sup>

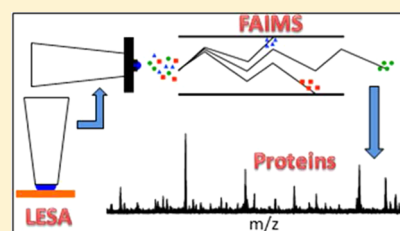
<sup>†</sup>School of Biosciences, University of Birmingham, Edgbaston, Birmingham B15 2TT, United Kingdom

<sup>‡</sup>National Physical Laboratory, Hampton Road, Teddington, Middlesex TW11 0LW, United Kingdom

<sup>§</sup>School of Pharmacy, University of Nottingham, University Park, Nottingham NG7 2RD, United Kingdom

## S Supporting Information

**ABSTRACT:** Previously we have shown that liquid extraction surface analysis (LESA) mass spectrometry is suitable for the analysis of intact proteins from a range of biological substrates. Here we show that LESA mass spectrometry may be coupled with high field asymmetric waveform ion mobility spectrometry (FAIMS) for top-down protein analysis directly from thin tissue sections (mouse liver, mouse brain) and from bacterial colonies (*Escherichia coli*) growing on agar. Incorporation of FAIMS results in significant improvements in signal-to-noise and reduced analysis time. Abundant protein signals are observed in single scan mass spectra. In addition, FAIMS enables gas-phase separation of molecular classes, for example, lipids and proteins, enabling improved analysis of both sets of species from a single LESA extraction.



Liquid extraction surface analysis (LESA)<sup>1</sup> mass spectrometry is emerging as a powerful tool for in situ analysis of intact proteins. In LESA, a robotic pipet dispenses a droplet (a few  $\mu\text{L}$ ) of solvent onto the surface under investigation. The droplet is held in contact between the pipet and the surface for a few seconds, that is, a liquid microjunction is maintained, and soluble analytes are extracted. The sample droplet is reaspirated and introduced into the mass spectrometer via electrospray ionization. Edwards et al. demonstrated that the approach, which is also known as liquid microjunction sampling, could be applied to the analysis of hemoglobin variants from neonatal dried blood spots.<sup>2–4</sup> Schey et al. demonstrated manual LESA of intact proteins from thin tissue sections of mouse brain and kidney, and bovine ocular lens.<sup>5</sup> Sarsby et al. applied LESA mass spectrometry for the analysis of intact protein biomarkers of nonalcoholic liver disease.<sup>6</sup> More recently, we have shown that a variation of LESA, which we termed “contact” LESA allows top-down analysis of proteins from living bacterial colonies<sup>7</sup> and intact protein complexes.<sup>8</sup>

Challenges for top-down protein analysis by LESA mass spectrometry include those faced in any top-down electrospray analysis—the requirement for high resolution mass spectrometry, the presence of multiple charge states (for both precursor and fragment ions), the large number of fragmentation channels available. These challenges are compounded in LESA mass spectrometry by the potential complexity of the sample, particularly for biological substrates. Multiple proteins and proteoforms may be present over a wide dynamic range. In addition, the presence of other molecular classes, for example, lipids, may cause interference as a result of ion suppression. To

date, LESA MS of proteins tends to involve collection and coadding of multiple scans in order to obtain sufficient S/N for peak detection. This feature could present a barrier to the adoption of LESA MS for imaging of intact proteins. A potential solution to the issue of sample complexity is the coupling of liquid-phase separation methods; however, this brings a significant time cost. A typical HPLC MS analysis takes  $\sim 1$  h,<sup>5</sup> clearly incompatible with fast acquisition of a LESA image even of relatively few pixels. In contrast, the gas-phase separation afforded by ion mobility spectrometry, which separates ions on the basis of shape and charge, can be achieved on the order of milliseconds.

High-field asymmetric waveform ion mobility spectrometry (FAIMS), also known as differential ion mobility spectrometry, offers several advantages for the analysis of peptides and proteins, including reduced chemical noise, improved S/N,<sup>9–12</sup> and separation of peptide isomers.<sup>13–16</sup> FAIMS separates gas-phase ions at atmospheric pressure on the basis of differences in the ion mobilities in high and low electric fields.<sup>17,18</sup> Ions are passed between two parallel electrodes by a carrier gas. An asymmetric waveform is applied to the electrodes to provide alternating high and low electric fields perpendicular to the direction of the ions' trajectory through the device. The high electric field is designated the dispersion field (DF). As a result of the differences in mobilities in high and low electric fields, the ions will deviate from their original trajectory toward one of

Received: March 12, 2015

Accepted: June 11, 2015

Published: June 11, 2015

the electrodes. If uncorrected, they will collide with the electrode. Superposition of a compensation field (CF) prevents this occurrence. By tuning the compensation field, it is possible to selectively transmit ions of a particular differential mobility.

FAIMS devices have previously been coupled to ambient ionization techniques for the analysis of small molecules. Fernandez and co-workers coupled desorption electrospray (DESI) with FAIMS for the analysis of counterfeit pharmaceuticals.<sup>19</sup> More recently, they demonstrated DESI FAIMS mass spectrometry for the imaging of phosphatidylcholines ( $m/z$  700–900) in rat brain tissue.<sup>20</sup> Manicke and Belford coupled paperspray ionization with FAIMS for the separation of isomeric drug compounds.<sup>21</sup> Porta and co-workers have shown that LESA coupled with FAIMS is suitable for the analysis of drugs of abuse and their metabolites.<sup>22</sup> In that work, a prototype FAIMS device was coupled with a triple quadrupole linear ion trap mass spectrometer.

Here, we demonstrate the benefits of FAIMS for intact and top-down protein analysis by LESA mass spectrometry. We have coupled LESA with a miniaturized chip-based FAIMS device<sup>23</sup> and a high resolution orbitrap mass spectrometer. LESA FAIMS analyses were performed on thin tissue sections from mouse liver and mouse brain and on *E. coli* colonies growing on agar (Note, the analysis of bacteria made use of the “contact” LESA approach described in ref 7). The results show significant improvements in protein peak S/N, enabling detection of proteins in single scan mass spectra (i.e., in under 2 s, compared with several minutes required in the absence of FAIMS). Moreover, it is possible to separate molecular classes such that different species may be analyzed from a single LESA extraction. That is, FAIMS addresses the inherent challenge of sample complexity in LESA MS of biological substrates.

## ■ EXPERIMENTAL SECTION

**Materials.** *Thin Tissue Sections.* Liver and brain from wild-type mice (extraneous tissue from culled animals) were the gift of Prof. Steve Watson (University of Birmingham). Organs were frozen on dry ice prior to storage at  $-80$  °C. Sections of murine liver tissue and brain tissue of area  $\sim 1.5$  cm<sup>2</sup> were obtained at a thickness of 10  $\mu$ m using a CM1810 Cryostat (Leica Microsystems, Wetzlar, Germany) and thaw mounted onto glass slides.

*E. coli* Colonies. A strain of *Escherichia coli* K-12 was inoculated onto solid LBA medium (LB 20 g L<sup>-1</sup> Agar 20 g L<sup>-1</sup>) in 6 cm diameter Petri dishes. Samples were incubated at 37 °C for  $\sim 12$  h and subsequently stored in the dark at 4 °C until analysis ( $\sim 43$  days).

*Solvents.* The following solvents were used: acetonitrile (J. T. Baker, The Netherlands), methanol (J. T. Baker, The Netherlands), ethanol (Fisher Scientific, Loughborough, U.K.), HPLC grade water (J. T. Baker, The Netherlands), and formic acid (Sigma-Aldrich Company Ltd., Dorset, U.K.).

*Peptide and Protein Standards (for direct infusion electrospray).* A solution comprising AAAAAAnYK (2  $\mu$ M; nY = nitrotyrosine; AltaBioscience, Birmingham, U.K.) and angiotensin I (2  $\mu$ M), substance P (2  $\mu$ M), bovine ubiquitin (5  $\mu$ M), and hemoglobin S (5  $\mu$ M) (all Sigma-Aldrich, Dorset, U.K.) was prepared in 69.5:29.5:1 methanol/water/formic acid.

**Liquid Extraction Surface Analysis.** Thin tissue section samples were loaded onto a universal LESA adapter plate and placed in the TriVersa Nanomate chip-based electrospray device (Advion, Ithaca, NY) coupled to the Thermo Fisher

Scientific Orbitrap Velos or Elite (Thermo Fisher Scientific, Bremen, Germany). Bacteria samples were placed directly in the TriVersa Nanomate (see ref 7 for details).

*Thin Tissue Sections.* The solvent system used for LESA extraction/electrospray was 69.5:29.5:1 methanol/water/formic acid (mouse liver) or 39.5:59.5:1 acetonitrile/water/formic acid (mouse brain). Brain sections were prewashed by LESA sampling with 80:20 ethanol/water. Wash solutions were dispensed to waste. A total of 6  $\mu$ L were aspirated from the solvent well. The robotic arm relocated to a position above the tissue and descended to a height 0.2 mm above the surface of the sample. A total of 3  $\mu$ L of the solution was dispensed onto the sample surface to form a liquid microjunction. The liquid microjunction was maintained for 10 s; then 3.5  $\mu$ L were reaspirated into the pipet tip.

*E. coli.* The solvent system used for LESA extraction/electrospray was 39.5:59.5:1 acetonitrile/water/formic acid. Three  $\mu$ L were aspirated from the solvent well. The robotic arm relocated to a position above the bacterial colony and descended until in contact with the surface of the bacterial colony. A total of 2  $\mu$ L of the solution was dispensed onto the sample surface to form a liquid microjunction. The liquid microjunction was maintained with the surface for 3 s; then 2.5  $\mu$ L were reaspirated into the pipet tip.

Samples were introduced into the mass spectrometer via the TriVersa NanoMate, with gas pressure 0.3 psi, a tip voltage of 1.75 kV (or 1.55 kV for direct infusion electrospray), and a capillary temperature of 250 °C.

**UltraFAIMS.** The TriVersa Nanomate was coupled to a miniaturized ultra-FAIMS device (Owlstone, Cambridge, U.K.), which was coupled to an Orbitrap Velos or Orbitrap Elite mass spectrometer (Thermo Fisher Scientific, Bremen Germany), see Supporting Information, Figure 1. FAIMS separation was carried out in positive ion mode using a microchip device (Owlstone).<sup>24</sup> The FAIMS device was operated either in 2D mode or in static mode.

*2-D FAIMS Analyses.* FAIMS separation was carried out at eight discrete dispersion fields (DFs) between 130 and 270 Td with a step size of 20 Td. At each DF, the compensation field was varied between  $-1$  to  $+4$  Td (step size 2.5 mTd) over a time period of 180 s.

*Static FAIMS Analyses.* Optimal DF and CF conditions for the transmission of ions of interest were selected from the 2D FAIMS analyses. Data shown were recorded as follows: Mouse Liver: DF = 130 Td, CF = 0.30 Td. Mouse brain: DF = 270 Td, CF = 2.60 Td. *E. coli*: DF = 210 Td, CF = 1.65 Td.

**Mass Spectrometry.** The majority of mass spectrometry experiments were performed on a Thermo Fisher Orbitrap Velos. Results shown for the 2D FAIMS analysis of mouse brain sections were recorded on a Thermo Fisher Orbitrap Elite.

Mass spectra were collected in full scan mode ( $m/z$  400–2000 (mouse samples);  $m/z$  500–2000 (*E. coli* samples)) at a resolving power of 100000 at  $m/z$  400 (Orbitrap Velos) or 120000 (Orbitrap Elite) at  $m/z$  200. The AGC target was  $1 \times 10^6$  charges with a maximum injection time of 1000 ms. Each scan was composed of 1 microscan.

*Tandem Mass Spectrometry.* CID: CID was carried out in the linear ion trap at normalized collision energy of 30%, and fragment ions were detected in the orbitrap at a resolving power of 100000 at  $m/z$  400. AGC target was  $1 \times 10^6$  (mouse tissue samples) or  $1 \times 10^5$  (*E. coli* samples) with maximum injection time of 1 s. HCD: HCD experiments (NCE 30%)

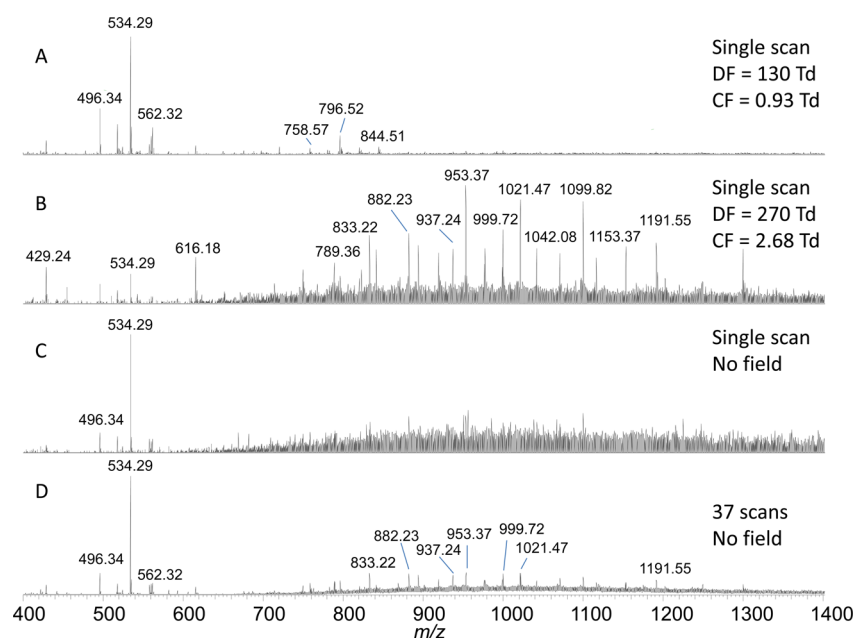


**Figure 1.** LESA 2D-FAIMS mass spectrometry of mouse liver. (A) Single scan mass spectrum at DF = 130 Td, CF = 0.93 Td; (B) Single scan mass spectrum at DF = 270 Td, CF = 2.68 Td; (C) Single scan mass spectrum recorded in the absence of FAIMS field; (D) Mass spectrum recorded in the absence of FAIMS field comprising 37 coadded scans (~1 min data).

were recorded at a resolving power of 100000 at  $m/z$  400. AGC target was  $1 \times 10^6$  (mouse tissue samples) or  $1 \times 10^5$  (*E. coli* samples) with maximum injection time of 1 s. ETD: ETD was performed with fluoranthene ions. AGC target for precursor ions was  $1 \times 10^6$  with maximum injection time 1 s. AGC target for fluoranthene ions was  $1 \times 10^6$  (maximum inject time 1 s). Precursor ions were activated for 30 ms. For all fragmentation methods, isolation widths were 3 Th ( $m/z$  1021.54 from liver), 7.5 Th ( $m/z$  952.63 from brain), and 10 Th ( $m/z$  1392.27 from *E. coli*). MS/MS spectra were comprised of five microscans. Data were recorded for 2–5 min in each case.

Data were analyzed using either Xcalibur version 2.1.0.1139 or 3.0.63 software.

## DATA ANALYSIS

**Visualization of FAIMS Data.** Data were converted from Thermo.raw format to mzML using msconvert as part of ProteoWizard<sup>25</sup> and then to imzML using imzMLConverter.<sup>26</sup> Data in the imzML format were then loaded into MATLAB (version 2013, The MathWorks Inc., Natick, Massachusetts) using imzMLConverter and in-house software.

**Total Ion Transmission Maps.** A linear  $m/z$  axis was generated between  $m/z$  500 and 2000 with a step interval of 0.5. Generation of total ion transmission maps were performed by sequentially loading in each spectrum from the 2D FAIMS analysis, summing all data points that fell between adjacent intervals on the linear  $m/z$  axis and inserting into a 2D matrix ( $m \times n$ , where  $m$  is number of scans in the 2D FAIMS analysis and  $n$  is number of  $m/z$  bins on the generated  $m/z$  axis). Isolation and display of a single DF value was performed by extracting the relevant scans from the full data matrix and normalizing to CF.

**Single Ion Transmission Maps.** Selected  $m/z$  values (with user defined tolerance) from the 2D FAIMS analysis were loaded into an array. Generation of single ion transmission maps was performed by selecting scans from each DF value, and projecting signal intensities of the selected  $m/z$  into a 2D

matrix ( $m \times n$ , where  $m$  is the CF (normalized to scan number) and  $n$  is the DF). The 2D matrix was displayed in false color normalized to the maximum intensity of the ion.

Software for generation of total ion transmission maps and single ion transmission maps, together with a step-by-step guide, is available for download from <http://www.biosciences-labs.bham.ac.uk/cooper/software.html>.

**Analysis of MS/MS Data.** All mass spectra were deconvoluted using the Xtract function in Xcalibur in order to obtain monoisotopic masses. Mass spectra were processed with a signal-to-noise ratio threshold of three. The processed fragment ion list was submitted to ProSight PTM 2.0 (<https://prosigthptm2.northwestern.edu>) and searched against the mouse or *E. coli* K-12 database accordingly, allowing all modifications, with a fragment tolerance of 10 ppm. Identity was confirmed by manual analysis using Protein Prospector (<http://prospector.ucsf.edu/prospector/mshome.htm>).

## RESULTS AND DISCUSSION

The miniaturized chip-based ultraFAIMS device was coupled with the orbitrap mass spectrometer and the Triversa Nanomate, see Supporting Information, Figure 1. LESA FAIMS mass spectrometry analyses, in which both the dispersion field (DF) and the compensation field (CF) were varied (2D FAIMS analysis), were performed on thin tissue sections from mouse liver and mouse brain and on *E. coli* growing on agar. Optimal DF and CF conditions for the transmission of a particular species of interest were determined and static FAIMS analyses, at a single DF and single CF setting, were conducted. Static FAIMS analyses were coupled with tandem mass spectrometry for protein identification.

The transmission efficiency through the ultraFAIMS device is illustrated in Supporting Information, Figure 2. The figure shows single scan mass spectra of substance P and ubiquitin following direct infusion electrospray of a peptide/protein mixture (i.e., no LESA). In each case, the top mass spectrum was recorded in the absence of the FAIMS device, the middle

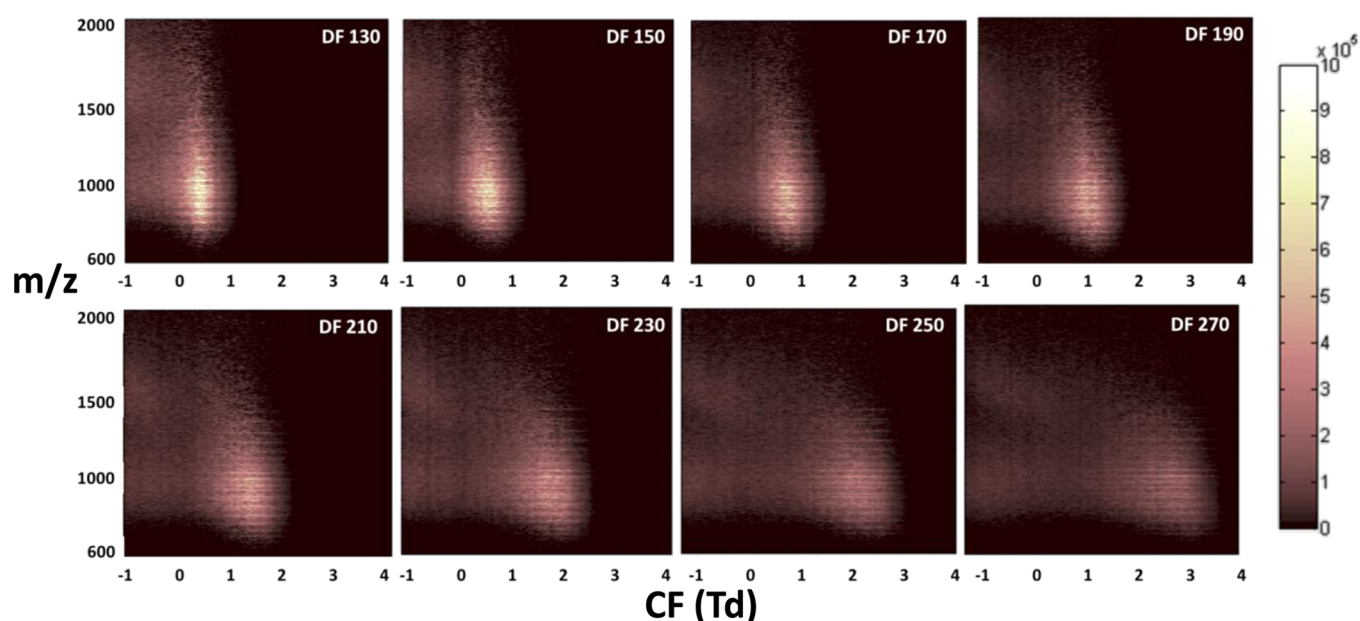


**Figure 2.** Total ion transmission maps obtained following LESA 2D FAIMS analyses of mouse liver.

mass spectrum was recorded with the FAIMS device coupled but with no field applied, and the bottom mass spectrum was recorded at the optimum FAIMS conditions for the ions of interest. The results show that, while there is a drop in sensitivity ( $\sim 1$  order of magnitude) as a result of coupling the FAIMS device, once coupled, the transmission efficiency (FAIMS field applied vs FAIMS no field) is  $\sim 80\%$ . Moreover, with FAIMS field applied the signal-to-noise improves  $\sim 2$ -fold and  $\sim 14$ -fold for the monoisotopic peaks of substance P and ubiquitin, respectively.

**2D FAIMS Analyses.** Incorporation of FAIMS into the LESA workflow resulted in improved signal-to-noise for both intact protein peaks and small singly charged species. Figure 1A,B shows mass spectra obtained during a 2-D sweep of dispersion field (DF) and compensation field (CF) following LESA sampling of thin tissue sections of mouse liver. Each mass spectrum represents a single scan, that is, total MS analysis time of 1.8 s. At DF = 130 Td and CF = 0.93 Td (Figure 1A), the mass spectrum is dominated by peaks corresponding to singly charged small molecules. The abundant peaks at  $m/z$  534.29 and 496.34 correspond to lysophosphatidylcholine (lyso-PC) 16:0  $[M + K]^+$  and  $[M + H]^+$  adducts, respectively. Abundant peaks at  $m/z$  796.52 and 758.57 correspond to phosphatidylcholine PC 34:2  $[M + K]^+$  and  $[M + H]^+$  adducts, respectively. At DF = 270 Td and CF = 2.68 Td, the mass spectrum is dominated by peaks corresponding to intact protein ions, notably  $\alpha$ - and  $\beta$ -globin ( $\sim 15$  and  $\sim 16$  kDa, respectively) and fatty acid binding protein FABP1 ( $\sim 15$  kDa; see below). For comparison, a single scan mass spectrum in the absence of FAIMS field is shown in Figure 1C and a 1 min data summation (37 scans) in Figure 1D. After coadding 37 scans, the S/N of the peak at  $m/z$  953 is 14. The same peak in the single FAIMS MS spectrum (Figure 1B) has S/N of 50. Similar results were obtained following LESA FAIMS analysis of mouse brain and *E. coli*, see Supporting Information, Figures 3 and 4. For the mouse brain sample, dominant peaks corresponding to an unknown protein of  $\sim 22$  kDa were observed, including in the absence of the FAIMS field. Nevertheless, at certain FAIMS parameters, for example, DF = 270 Td, CF = 3.32 Td

(Supporting Information, Figure 3A), 17 proteins in the molecular weight range 1–9 kDa were observed.

The results obtained from a 2D FAIMS analysis inform on the gas-phase separation achieved and the optimum FAIMS conditions (DF and CF) for transmission of a particular molecular ion. Figure 2 shows the total ion transmission maps obtained from the LESA FAIMS analysis of mouse liver. The distribution of observed  $m/z$  with compensation field at each of the dispersion fields is shown. As DF increases, greater separation with CF is observed. Three notable regions emerge. Consider the results at DF = 270 Td. In the region CF = 1.5–3.5 Td and  $m/z \sim 700$ –1500, proteins in the molecular weight range 14–23 kDa are transmitted. (The mass spectrum shown in Figure 1B corresponds to this region of the FAIMS space.) A second cluster is apparent in the region CF =  $-0.5$ –1 Td and  $m/z \sim 800$ –1100, and a third in the region CF =  $-0.5$ –1 Td and  $m/z \sim 1400$ –1900. The species in these clusters correspond to high molecular weight (unresolved) proteins, see Supporting Information, Figure 5.

The separation of lower and higher molecular weight proteins is in agreement with the work of Shvartsburg and co-workers.<sup>27–29</sup> Shvartsburg et al.<sup>27</sup> showed that whereas smaller proteins displayed type C behavior<sup>18</sup> (i.e., ion mobility decreases with electric field strength), proteins with molecular weight  $>30$  kDa showed an increase in ion mobility with electric field strength (A- or B-type behavior<sup>18</sup>). This observation was attributed to alignment of the protein dipole for the larger proteins with the electric field during the high field portion of the FAIMS cycle (generally, dipole moment scales with protein size). As a result, the collision cross section of the protein ion in the plane orthogonal to the dipole moment, rather than the rotationally averaged collision cross section, dictates the ion mobility. Further work<sup>28</sup> suggested that the minimum dipole moment required for alignment in any field was  $\sim 450$  D, corresponding to a protein of MW  $\sim 30$  kDa. The hypothesis was validated using the ultrahigh field FAIMS devices used in the current work:<sup>29</sup> Ubiquitin ions ( $\sim 8.6$  kDa) displayed C-type behavior, that is, did not align, whereas bovine serum albumin ( $\sim 66$  kDa) displayed A-type behavior, that is,

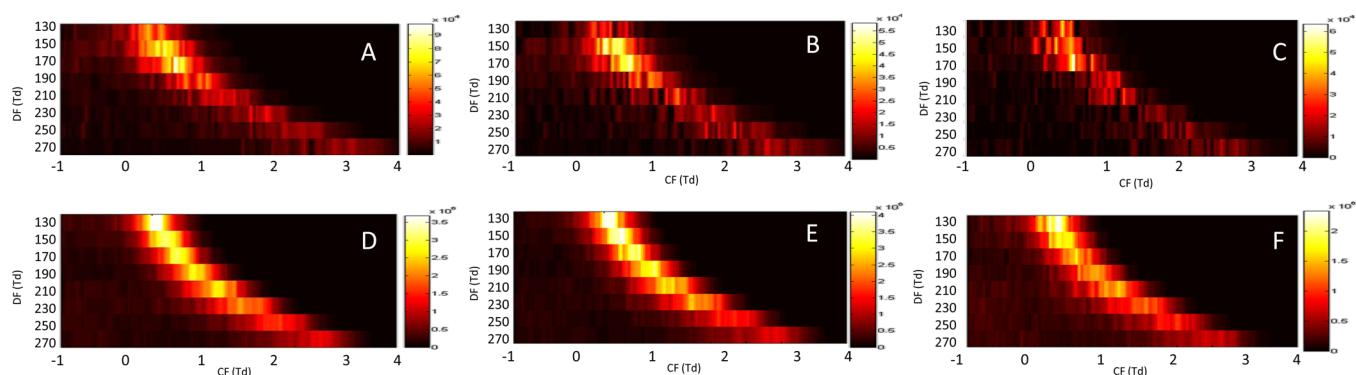


**Figure 3.** Ion transmission maps for specific  $m/z$  following LESA 2D FAIMS analyses of mouse liver (A)  $m/z$  758.57  $\pm$  0.01 (PC(34:2) + H<sup>+</sup>); (B)  $m/z$  760.58  $\pm$  0.01 (PC(34:1) + H<sup>+</sup>); (C)  $m/z$  806.57  $\pm$  0.01 (PC(38:6) + H<sup>+</sup>); (D)  $m/z$  919.7  $\pm$  1.0 ( $\beta$ -globin, +17 charge state); (E)  $m/z$  882.7  $\pm$  1.0 ( $\alpha$ -globin, +17 charge state); (F)  $m/z$  894.0  $\pm$  1.0 (fatty acid binding protein FABP1, +16 charge state).

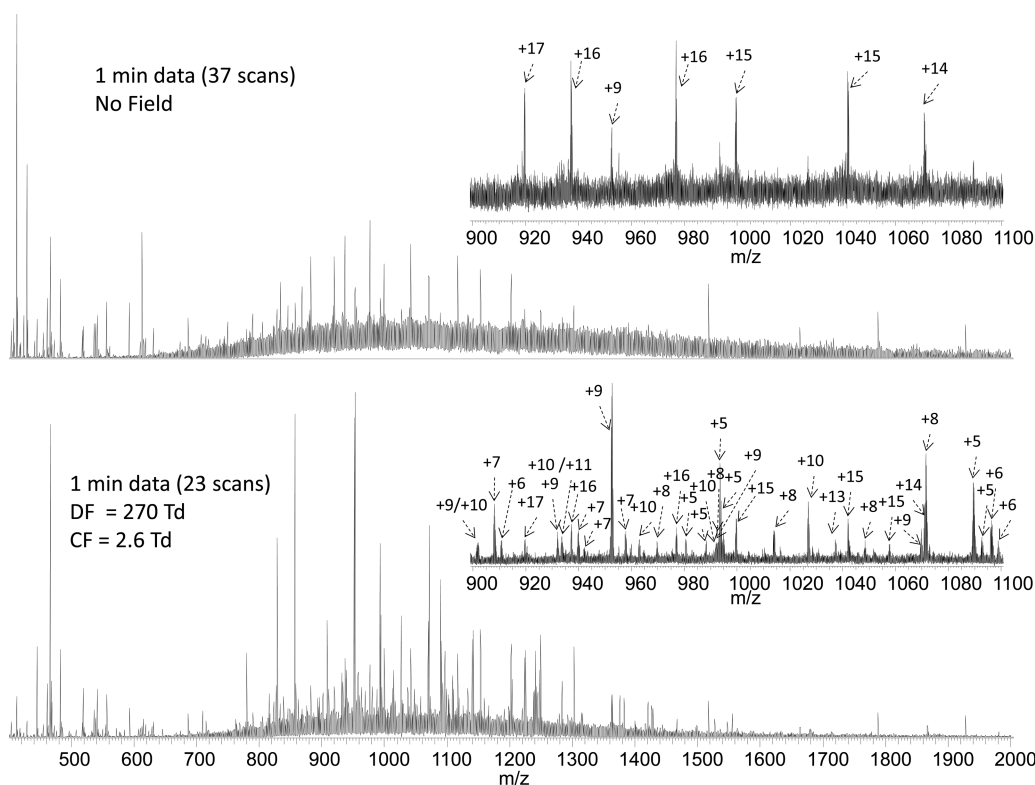


**Figure 4.** LESA FAIMS mass spectrometry of mouse brain: static FAIMS mode. (Top) LESA mass spectrum obtained in the absence of FAIMS field. (Bottom) LESA FAIMS mass spectrum obtained at DF = 270 Td, CF = 2.6 Td. Inset: Expanded  $m/z$  regions. Both mass spectra comprise 1 min of data.

dipoles aligned. In the experiments described here, the high field portion of the FAIMS cycle (the dispersion field) varies between  $\sim 30$  kV/cm (130 Td) and  $\sim 70$  kV/cm (270 Td), and dipole alignment of the higher molecular weight protein ions is expected. That is, the improved signals observed here for proteins are the result of the separation of higher molecular weight A-type protein ions and the lower molecular weight C-type protein ions.

The total ion transmission maps obtained following LESA 2D-FAIMS MS analyses of mouse brain and *E. coli* are shown in Supporting Information, Figure 6. Similar trends were observed in both cases. As discussed, this particular mouse brain sample is dominated by the presence of an unknown protein of  $\sim 22$  kDa, and this feature is apparent in the total ion transmission maps. Nevertheless, higher molecular weight proteins ( $\sim 30$

kDa) were transmitted at lower compensation fields, whereas lower molecular weight proteins ( $\sim 10$  kDa) were transmitted at higher compensation fields (see Supporting Information, Figure 3). For all samples, the total ion transmission maps have a striated appearance. These striations arise from the various charge states of the proteins.

Figure 3 shows ion transmission maps for specific  $m/z$  values. Figure 3A–C shows maps obtained following analysis of mouse liver for  $m/z$  758.57, 760.58, and 806.57 corresponding to protonated lipids phosphatidylcholine PC(34:2), PC(34:1), and PC(38:6), respectively. The results suggest that, for these species, the optimum FAIMS parameters are dispersion fields of 150–170 Td and compensation fields between 0 and 1 Td. At higher dispersion fields, the lipids are transmitted at higher compensation fields.

Figures 3D–F shows the transmission maps for three proteins from mouse liver. Transmission maps for ions of  $m/z$  919.7, 882.7, and 894.0, corresponding to  $\beta$ -globin (+17 charge state),  $\alpha$ -globin (+17 charge state), and liver fatty acid binding protein FABP1 (+16 charge state), respectively, are shown. The data show that for proteins  $\alpha$ - and  $\beta$ -globin in the 17+ charge state, optimum transmission occurs at DF = 130 Td and CF  $\sim$  0.65 Td. Similar conditions were optimal for FABP1 in the 16+ charge state.

**Static FAIMS Analyses.** Optimum CF and DF conditions were identified for the maximum transmission (and separation) of proteins of interest by interrogating the results of 2D FAIMS analyses. These conditions were subsequently applied for static FAIMS analyses. Figure 4 shows results obtained following LESA of a mouse brain section in the absence of FAIMS field and in a static FAIMS analysis (DF = 270 Td, CF = 2.6 Td). (Note, this sample is separate from that described above and is not dominated by the 22 kDa protein.) Both mass spectra represent 1 min of data collection (a total of 37 scans for the non-FAIMS analysis and 23 scans with FAIMS applied). Clearly, the LESA FAIMS mass spectrum is far richer in information than the spectrum obtained without FAIMS. In this example, the majority of the peaks in the non-FAIMS spectrum correspond to  $\alpha$ -globin and  $\beta$ -globin in charge states +19 to +12, with an additional +9 peak at  $m/z$  952.63, that is, three proteins were detected. It may be that in this analysis a blood vessel on the tissue surface was sampled. In contrast, the FAIMS mass spectrum reveals peaks corresponding to numerous protein species (total of 29 individual protein masses) in the range  $\sim$ 5 to  $\sim$ 37 kDa in a range of charge states, and the globins are not the most abundant species.

The use of static FAIMS conditions enables tandem mass spectrometry of the intact proteins. Supporting Information, Figure 7, shows LESA FAIMS MS/MS spectra for ions with  $m/z$  1021.54 (+14 charge state; DF = 130 Td, CF = 0.30 Td) from mouse liver and  $m/z$  952.63 (+9 charge state; DF = 270 Td, CF = 2.60 Td) from mouse brain. Note that static FAIMS conditions are optimized for both maximum transmission and separation of ions of interest from other species and, therefore, depend on the complexity of the substrate. Thus, the optimum CF and DF values differ between the liver and brain samples (and *E. coli* samples below). Collision-induced dissociation (CID), higher energy collision dissociation (HCD), and electron transfer dissociation (ETD) were performed. The data were searched against a mouse protein database using the ProSight software to obtain putative assignments. The fragment ions were subsequently manually analyzed and protein identifications confirmed. The proteins were identified as liver fatty acid binding protein (FABP1) and ubiquitin. A similar analysis was performed on a protein from the *E. coli* sample. Ions of  $m/z$  1392.27 (+7 charge state; DF = 210 Td, CF = 1.65 Td) were selected for CID. The MS/MS spectrum and fragment ion summary are shown in Supporting Information, Figure 8. The protein was identified as acid stress chaperone HdeA. This protein has not previously been identified following LESA of *E. coli* colonies.

## CONCLUSION

We have shown that high resolution LESA mass spectrometry may be coupled with FAIMS for the analysis of intact proteins from a range of biological substrates. The approach has been demonstrated on thin tissue sections from liver and brain and on bacterial colonies growing on agar. Improvements in S/N

were observed due to the separation of higher molecular weight proteins and small singly charged species from proteins of lower molecular weight. These improvements in S/N result in shorter analysis times making FAIMS a potentially promising approach for intact protein imaging by LESA.

Various operating modes are available. It is possible to determine optimum FAIMS conditions through 2-D sweeps of dispersion field and compensation field and visualization of separation in the  $m/z$ /CF and in the DF/CF space. Optimum conditions (DF and CF) can subsequently be utilized in static FAIMS analysis which may be coupled with tandem mass spectrometry (CID, HCD, or ETD) for protein identification.

## ASSOCIATED CONTENT

### Supporting Information

Photographs of experimental setup; LESA-FAIMS mass spectra; LESA-FAIMS MS/MS spectra; total ion transmission maps from LESA-FAIMS analyses. The Supporting Information is available free of charge on the ACS Publications website at DOI: 10.1021/acs.analchem.5b01151.

## AUTHOR INFORMATION

### Corresponding Author

\*E-mail: h.j.cooper@bham.ac.uk.

### Notes

The authors declare no competing financial interest.

## ACKNOWLEDGMENTS

H.J.C. is an EPSRC Established Career Fellow (EP/L023490/1). J.S. and E.C.R. received funding from the EPSRC via the PSIBS doctoral training centre (EP/F50053X/1). E.C.R.'s studentship is in collaboration with Astra Zeneca and the National Physical Laboratory. The Advion Triversa Nanomate and Thermo Fisher Orbitrap Velos mass spectrometer used in this research were funded through Birmingham Science City Translational Medicine, Experimental Medicine Network of Excellence Project, with support from Advantage West Midlands. Supplementary data supporting this research is openly available from the University of Birmingham data archive at <http://findit.bham.ac.uk/>.

## REFERENCES

- (1) Kertesz, V.; Van Berkel, G. J. *J. Mass Spectrom.* **2010**, *45* (3), 252–260.
- (2) Edwards, R. L.; Creese, A. J.; Baumert, M.; Griffiths, P.; Bunch, J.; Cooper, H. J. *Anal. Chem.* **2011**, *83*, 2265–2270.
- (3) Edwards, R. L.; Griffiths, P.; Bunch, J.; Cooper, H. J. *Proteomics* **2014**, *14* (10), 1232–1238.
- (4) Edwards, R. L.; Griffiths, P.; Bunch, J.; Cooper, H. J. *J. Am. Soc. Mass Spectrom.* **2012**, *23*, 1921–1930.
- (5) Schey, K. L.; Anderson, D. M.; Rose, K. L. *Anal. Chem.* **2013**, *85* (14), 6767–6774.
- (6) Sarsby, J.; Martin, N. J.; Lalor, P. F.; Bunch, J.; Cooper, H. J. *J. Am. Soc. Mass Spectrom.* **2014**, *25* (11), 1953–1961.
- (7) Randall, E. C.; Bunch, J.; Cooper, H. J. *Anal. Chem.* **2014**, *86* (21), 10504–10510.
- (8) Martin, N. J.; Griffiths, R. L.; Edwards, R. L.; Cooper, H. J. *J. Am. Soc. Mass Spectrom.* **2015**, DOI: 10.1007/s13361-015-1152-8.
- (9) Guevremont, R.; Barnett, D. A.; Purves, R. W.; Vandermey, J. *Anal. Chem.* **2000**, *72*, 4577–4584.
- (10) Barnett, D. A.; Ells, B.; Guevremont, R.; Purves, R. W. *J. Am. Soc. Mass Spectrom.* **2002**, *13*, 1282–1291.
- (11) Venne, K.; Bonnell, E.; Eng, K.; Thibault, P. *Anal. Chem.* **2005**, *77*, 2176–2186.

- (12) Creese, A. J.; Shimwell, N. J.; Larkins, K. P. B.; Heath, J. K.; Cooper, H. J. *J. Am. Soc. Mass Spectrom.* **2013**, *24*, 431–443.
- (13) Creese, A. J.; Cooper, H. J. *Anal. Chem.* **2012**, *84*, 2597–2601.
- (14) Shvartsburg, A. A.; Creese, A. J.; Smith, R. D.; Cooper, H. J. *Anal. Chem.* **2010**, *82*, 8327–8334.
- (15) Shvartsburg, A. A.; Creese, A. J.; Smith, R. D.; Cooper, H. J. *Anal. Chem.* **2011**, *83*, 6918–6923.
- (16) Xuan, Y.; Creese, A. J.; Horner, J. A.; Cooper, H. J. *Rapid Commun. Mass Spectrom.* **2009**, *23*, 1963–1969.
- (17) Guevremont, R. J. *Chromatogr. A* **2004**, *1058*, 3–19.
- (18) Purves, R. W.; Guevremont, R.; Day, S.; Pipich, C. W.; Matyjaszczyk, M. *Rev. Sci. Instrum.* **1998**, *69*, 4094.
- (19) Galhena, A. S.; Harris, G. A.; Kwasnik, M.; Fernandez, F. M. *Anal. Chem.* **2010**, *82* (22), 9159–9163.
- (20) Bennett, R. V.; Gamage, C. M.; Galhena, A. S.; Fernandez, F. M. *Anal. Chem.* **2014**, *86*, 3756–3763.
- (21) Manicke, N. E.; Belford, M. J. *J. Am. Soc. Mass Spectrom.* **2015**, *26*, 701–705.
- (22) Porta, T.; Varesio, E.; Hopfgartner, G. *Anal. Chem.* **2013**, *85*, 11771–11779.
- (23) Shvartsburg, A. A.; Tang, K.; Smith, R. D.; Holden, M.; Rush, M.; Thompson, A.; Toutoungi, D. *Anal. Chem.* **2009**, *81* (19), 8048–8053.
- (24) Shvartsburg, A. A.; Smith, R. D.; Wilks, A.; Koehl, A.; Ruiz-Alonso, D.; Boyle, B. *Anal. Chem.* **2009**, *81* (15), 6489–6495.
- (25) Chambers, M. C.; Maclean, B.; Burke, R.; Amodoi, D.; Ruderman, D. L.; Neumann, S.; Gatto, L.; Fischer, B.; Pratt, B.; Egertson, J.; Hoff, K.; Kessner, D.; Tasman, N.; Shulman, N.; Frewen, B.; Baker, T. A.; Brusniak, M. Y.; Paulse, C.; Creasey, D.; Flashner, L.; Kani, K.; Moulding, C.; Seymour, S. L.; Nuwaysir, L. M.; Lefebvre, B.; Kuhlmann, F.; Roark, J.; Rainer, P.; Detlev, S.; Hemenway, T.; Huhmer, A.; Langridge, J.; Connolly, B.; Chadick, T.; Holly, K.; Eckels, J.; Deutsch, E. W.; Moritz, R. L.; Katz, J. E.; Agus, D. B.; Maccoss, M.; Tabb, D. L.; Mallick, P. *Nat. Biotechnol.* **2012**, *30*, 918–920.
- (26) Race, A. M.; Styles, I. B.; Bunch, J. J. *Proteomics* **2012**, *75* (16), 5111–5112.
- (27) Shvartsburg, A. A.; Bryskiewicz, T.; Purves, R. W.; Tang, K.; Guevremont, R.; Smith, R. D. *J. Phys. Chem. B* **2006**, *110* (43), 21966–21980.
- (28) Shvartsburg, A. A.; Noskov, S. Y.; Purves, R. W.; Smith, R. D. *Proc. Natl. Acad. Sci. U.S.A.* **2009**, *106* (16), 6495–6500.
- (29) Shvartsburg, A. A.; Smith, R. D. *Anal. Chem.* **2012**, *84*, 7297–7300.